Telomeres control regulation of the human Telomerase (hTERT) gene through non-telomeric TRF2 and independent of Telomere looping

*Antara Sengupta,[1,2,4], Soujanya Vinayagamurthy[1,2,4], Drishti Soni[1,2,4], Rajlekha Deb[1,4], Ananda Kishore Mukherjee[1,2,4], Subhajit Dutta[1,2,4], Jushta Jaiswal[1,4], Mukta Yadav[1,2,4], Shalu Sharma[1,2,4], Sulochana Bagri[1,2,4], Shuvra Shekhar Roy[1,2,4], Ankita Singh[1,4], Divya Khanna[1,4], Amit Kumar Bhatt[1,4], Akshay Sharma[3], Suman Saurav[3], Rajender K Motiani[3], Shantanu Chowdhury[1,2,4,5, *]*

[1]Integrative and Functional Biology Unit, CSIR-Institute of Genomics and Integrative Biology, New Delhi 110025, India

[2]Academy of Scientific and Innovative Research (AcSIR), Ghaziabad 201002, India

[3]Laboratory of Calciomics and Systemic Pathophysiology (LCSP), Regional Centre for Biotechnology (RCB), Faridabad, Delhi-NCR, India.

[4]CSIR-Institute of Genomics and Integrative Biology, New Delhi 110025, India

[5]Lead contact

*Correspondence: shantanuc@igib.in

Abstract

Activation of human telomerase (hTERT) and resulting maintenance of telomeres is widely understood. Whether telomeres, on the other hand, influence *hTERT* regulation is relatively less studied. We found *hTERT* was transcriptionally up/down regulated depending on telomere length (TL), but independent of telomere looping. Cells from different tissues, engineered for either telomere elongation/shortening gave increase/decrease in *hTERT*, respectively. Temporal increase of TL, followed by decrease over days, resulted in induction and subsequent repression of *hTERT*, supporting the causal role of TL. Further confirmed by TL-dependent promoter activity from exogenously inserted *hTERT* reporter. Mechanistically, we show non-telomeric TRF2 binding at the *hTERT* promoter to be TL-dependent. Promoter bound TRF2 recruited the canonical PRC2-complex inducing repressor histone H3K27-trimethylation. Together, these reveal a heretofore unaddressed model of telomere homeostasis in telomerase-positive cells, where TL-dependent *hTERT* levels in turn maintain long/short telomeres. This might help better understand telomere-related physiologies like cancer, ageing and pluripotency.

Key words: Telomere length, *hTERT* transcription, TRF2, G-quadruplex, xenograft, epigenetic repressor complex, Arginine methylation

Introduction

Telomeres are nucleoprotein structures comprising guanine-rich DNA sequence at the end of linear chromosomes[1–3]. The catalytic subunit of the ribonucleoprotein telomerase, human telomerase reverse transcriptase (hTERT) is necessary for replicating telomeric repeats to maintain telomeres[4–6]. Most cancer cells, in contrast to normal adult somatic cells, maintain telomeres through reactivation of *hTERT* (~90% of cancers); alternative lengthening of telomeres (ALT) is used in other cases[7–10]. *hTERT* therefore is tightly regulated at the epigenetic, transcriptional and translational levels[11].

Role of *hTERT* in synthesis and maintenance of telomeres has been extensively studied[3,5,11–13]. Relatively recent work suggests how telomeres, on the other hand, might affect *hTERT* expression. Physical looping of telomeres to the *hTERT* loci (~1.2 Mb away) was shown to repress *hTERT* through Telomeric Position Effect-over-long-distance (TPE-OLD)[14,15]; loss of looping in short telomeres induced *hTERT*. Contextually notable is recent work on telomere-dependent regulation of genes remote from telomeres. First, non-telomeric binding of TRF2 was found to be extensive (>20000 sites), spread across the genome including promoters, and affected epigenetic regulation of genes[16,17]. Second, shortening or elongation of telomeres released or sequestered telomeric TRF2, respectively. Resulting increase/decrease in non-telomeric promoter TRF2 affected gene expression[17]. The telomeric sequestration-dependent partitioning of telomeric versus non-telomeric TRF2 was proposed as Telomere-Sequestration-Partitioning (TSP) model, linking global gene regulation to telomeres (Figure 1)[17–20]. Interestingly, we found promoter-bound TRF2, that was not associated with telomeres (or non-telomeric), repressed *hTERT*[21].

Here we asked if telomeres affected *hTERT* regulation by altering non-telomeric TRF2 binding at the *hTERT* promoter. TRF2 binding at the *hTERT* promoter increased with telomere shortening, and downregulated *hTERT*. Conversely, reduced promoter TRF2 on telomere elongation upregulated *hTERT*. Consistent with TSP described above. This was clear in multiple cell types engineered for either telomere elongation or

shortening. An artificially inserted *hTERT* promoter (>40 Mb from telomere) showed TRF2-dependent and telomere-sensitive regulation. For a temporal model, using doxycycline (dox) inducible cells we elongated telomeres, and stopped elongation after a desired time. TRF2 binding at the *hTERT* promoter decreased as telomeres elongated over several days, and increased again with telomere shortening when dox treatment was stopped. Together these show a mode of telomere-dependent regulation of *hTERT*, the sole enzyme necessary for synthesizing telomeres, revealing a cellular feedback machinery connecting telomeres and *hTERT* expression.

Results

Telomere elongation upregulates *hTERT* through non-telomeric TRF2

To test if telomere length (TL) of cells affected TRF2 occupancy at the *hTERT* promoter, we first elongated telomeres in cells under isogenic backgrounds (termed as Short Telomere, ST or Long Telomere, LT cells hereon). We used HT1080 fibrosarcoma cells (HT1080-ST) or the TL-elongated version HT1080-LT (from constitutive expression of *hTERT* and the RNA component *hTERC*; previously characterised by others and us, Methods)[17,22]. TL difference between HT1080-ST/LT was confirmed by flow cytometry (FACS) (Figure 2A). Chromatin-immunoprecipitation (ChIP) of TRF2 gave significantly reduced occupancy of TRF2 on the *hTERT* promoter in HT1080-LT compared to HT1080-ST cells while the overall TRF2 protein levels were similar (Figure 2B, Supplementary Figure 1A, ChIP-qPCR spanning 0-300 bp upstream of transcription start site (TSS)).

TRF2-dependent H3K27 trimethylation[17], including at the *hTERT* promoter[21], was reported earlier: we next checked if this was TL-sensitive at the *hTERT* promoter. With TL elongation, the H3K27me3 mark was significantly reduced in HT1080-LT relative to the ST cells (Figure 2C). As expected from reduced promoter H3K27 trimethylation *hTERT* transcription was enhanced by >50% in HT1080-LT relative to ST cells; 3'UTR-specific primers were used to distinguish from exogenously expressed *hTERT* (Figure 2D).

To rule out any effect of exogenous *hTERT* (HT1080-LT cells above) we sought to elongate telomeres in an *hTERT*-independent way. Using a reported method

telomeres were elongated in MDAMB231 breast cancer cells with guanine-rich telomeric repeat (GTR) oligonucleotides (characterised by others and us; termed MDAMB231-ST/LT; TL difference quantified using FACS; Figure 2A, TRF2 protein levels Supplementary Figure 1A)[17,23]. MDAMB231-LT cells had lower TRF2 binding at the *hTERT* promoter compared to MDAMB231-ST cells (Figure 2B). Accordingly, H3K27 trimethylation at the *hTERT* promoter was reduced and *hTERT* upregulated in MDAMB231-LT compared to MDAMB231-ST cells (Figure 2C-D). Together, TL-sensitive regulation of *hTERT* was consistent in both HT1080 and MDAMB231 cells on telomere elongation.

Telomere shortening increased promoter TRF2 suppressing *hTERT* expression

As an alternative model, instead of elongation we shortened TL in HCT116 colorectal carcinoma cells (with higher average TL (~5.6 kb) compared to HT1080 (~4.5 kb) or MDAMB231 (~3 kb) cells)[17,22,24]. Two different methods were used for TL shortening: (a) *hTERT*-independent, telomere-specific sgRNA guided CRISPR-Cas9 to trim telomeres or (b) depletion of the *hTERC* RNA (Methods, TLs in HCT116-ST/LT quantified using FACS; Figure 2A, TRF2 protein levels Supplementary Figure 1A). The ST cells in both TL shortened models had higher TRF2 binding on the *hTERT* promoter compared to the HCT116-LT cells (Figure 2B). Also, we found higher repressor H3K27me3 mark at the *hTERT* promoter, as expected from increased TRF2, in ST compared to its LT counterpart in both the HCT116 models (Figure 2C). As expected, increase in H3K27me3 repressor mark at the *hTERT* promoter resulted in significantly reduced *hTERT* expression in ST relative to the HCT116-LT cells (Figure 2D).

Previously, enhanced H3K27 trimethylation from TRF2-dependent binding of the RE1-silencing factor (REST) and EZH2 (the catalytic component of the PRC2 repressor complex) was noted at the *hTERT* promoter[21]. Here we asked if the TL-sensitive H3K27 trimethylation resulted from altered REST/EZH2 binding at the *hTERT* promoter using HT1080-ST/LT (TL elongated) or HCT116-ST/LT (*hTERC* knockdown, TL shortened) cells. ChIP of REST showed enhanced occupancy on the *hTERT* promoter in ST relative to HT1080-LT cells (Figure 2E Left panel). EZH2 binding was also higher at the *hTERT* promoter in ST in compared to HT1080-LT cells (Figure 2F Left panel). Similarly, increase in REST and EZH2 binding at the *hTERT* promoter in

ST relative to LT cells was clear in the HCT116-ST/LT (Figure 2E, F Right Panel). The *hTERT* transcript was further quantified using fluorescence *in situ* hybridization (FISH; Figure 2G). In HCT116, ST cells with higher TRF2 occupancy at *hTERT* promoter had lower *hTERT* mRNA compared to LT cells (Figure 2G).

Artificially inserted *hTERT* promoter is telomere sensitive

To further test TL-sensitive *hTERT* promoter activity we used a reporter cassette comprising 1300 bp of the *hTERT* promoter upstream of the *gaussia luciferase* (gluc) gene. The reporter was inserted at the CCR5 safe-harbour locus, 46 Mb away from the nearest telomere, using CRISPR in HEK293T cells (Figure 2H). TL in HEK293T cells was shortened using the Cas9-sgRNA method described earlier (Figure 2I, TRF2 protein levels Supplementary Figure 1B). Higher TRF2 binding at the inserted *hTERT* promoter in ST compared to the HEK293-LT cells was clear (ChIP-qRT primers specific to the CCR5-*hTERT* insert used; Figure 2H, J). Consistent with this, H3K27me3 deposition was relatively high in ST cells (Figure 2K), and the *hTERT* promoter driven gluc reporter activity was reduced in the ST relative to the LT cells (Figure 2L).

Together, these show TL-dependent *hTERT* regulation through non-telomeric TRF2 as a likely intrinsic mechanism independent from the chromatin state at the endogenous *hTERT* locus. Moreover, physical proximity of the endogenous *hTERT* (~1.2 Mb from telomere) was reported as the underlying reason behind telomere looping-dependent *hTERT* silencing[15]. This is unlikely here due to: (a) the CCR5 locus being >40 Mb way from telomere limits physical proximity; and (b) in the earlier study long telomeres promoted looping and consequent telomeric-heterochromatinization downregulated *hTERT*[15]. In contrast, we note longer TL give reduced TRF2 binding, open chromatin and increase in *hTERT*. Context-specific telomeric looping and/or non-telomeric mechanisms could be involved.

Temporally elongated or shortened telomeres up or downregulate *hTERT*

We next studied the effect of time-dependent (temporal) TL elongation/shortening, *i.e.*, TL increase followed by decrease in a continuous way. For this we made stable

HT1080 cells with doxycycline inducible *hTERT* (Dox-HT1080, Figure 3A). Induction of *hTERT*, and telomerase activity, resulted in gradual increase in TL to >3-fold by day-10; with discontinuation of dox after day-10 TL returned to the initial (day-0) state by day-24 (Figure 3B, Supplementary Figure 2A, TRF2 protein levels Supplementary Figure 2B left panel).

TRF2 binding at the *hTERT* promoter decreased gradually and significantly as TL increased up to day-10. Conversely, as TL decreased beyond day-10 TRF2 occupancy on the *hTERT* promoter increased and returned to almost day-0 levels (Figure 3C). Notably, this showed TRF2 binding at the *hTERT* promoter to be temporally controlled as a function of TL. Second, this further showed *hTERT* promoter-bound TRF2 was likely non-telomeric, because telomere-associated TRF2 would increase with TL elongation (and looping), instead of decrease seen here.

We then examined occupancy of REST and EZH2 at the *hTERT* promoter at days-0, 10 or 24: decrease in occupancy of both REST and EZH2 at day-10, relative to day-0, followed by increase at day-24 was clearly evident (Figure 3D and 3E). Accordingly, H3K27me3 deposition at the *hTERT* promoter was lower at day-10 compared to day-0, followed by increase at day-24 (Figure 3F). Taken together, clearly REST and EZH2 binding, and H3K27me3 occupancy were as expected from decrease/increase in TRF2 binding at the *hTERT* promoter as TL increased and then receded.

Consistent with this, expression of the endogenous *hTERT* (using 3'UTR qRT primers) increased at day-10 from day-0 levels, and reduced by day-24 (Figure 3G). Supporting the role of TL elongation in inducing or TL shortening in suppressing *hTERT*.

To exclude the possibility of cell-type specific effects, we considered a second temporal model using stable MDAMB231 cells with dox-inducible *hTERT* (Dox-MDAMB231; Figure 3H, Supplementary Figure 2A, B right panel). TL elongated to >2-folds by day-10; and receded to initial length by day-14 after stopping dox at day-10 (Figure 3I and Supplementary Figure 2A right panel). Significant decrease in TRF2 binding, and corresponding reduced H3K27me3 mark was clear at day-10 versus day-0 (Figure 3J and 3K). Further, both TRF2 and H3K27 trimethylation increased by day-14, as expected from TL shortening after day-10 (Figure 3J and 3K). The endogenous *hTERT* transcript followed TL elongation/shortening: increase at day-10 compared to day-0, and subsequent reduction at day-14 was clear (Figure 3L). Together, data from

two independent models of temporally altered TL, further supported promoter TRF2-binding mediated *hTERT* regulation to be TL-dependent.

Telomere-dependent *hTERT* regulation *in vivo* within xenograft tumours

We next sought to test TL-sensitive TRF2 binding at the *hTERT* promoter *in vivo.* Xenograft tumours were grown with either HT1080-ST or HT1080-LT cells in NOD/SCID mice (n=5 each, for tumour size characterization see Methods, Figure 4A). Following harvesting tumours were first characterised: TL was overall higher in all LT tumours compared to HT1080-ST tumours; increased *hTERT* and telomerase activity was retained in HT1080-LT tumours relative to ST, while TRF2 levels were comparable (Figure 4B, C; Supplementary Figure 3A, B). TRF2-ChIP from tumour tissue showed HT1080-ST had significantly more TRF2 occupancy at the *hTERT* promoter than HT1080-LT, consistent with results from cultured cells (Figure 4D and Figure 2B). Correspondingly, H3K27me3 mark deposition was reduced in xenograft HT1080-LT tumours compared to HT1080-ST (Figure 4E) supporting TL-dependent *hTERT* regulation was retained in cells growing *in vivo*.

G-quadruplex mediated TRF2 binding is essential for telomere-dependent *hTERT* regulation

G-quadruplex (G4) DNA secondary structures[25], widely reported as gene regulatory motifs[26–29], were found in the *hTERT* promoter[30,31]. G4-dependent promoter TRF2 binding was also recently shown to regulate *hTERT*[21]. Here we asked, whether and how TL-dependent *hTERT* regulation was affected by the promoter G4s. We used the *hTERT* promoter-*gluc*-reporter inserted at the CCR5 locus in HEK293T cells described above (Figure 2H). G>A mutations at -124 or -146 positions from TSS, frequently found to be clinically associated with multiple cancers and reported to disrupt the G4s[32–35], were introduced in the reporter (scheme in Figure 4A). Consistent with previous work[21], loss in TRF2 binding and H3K27 trimethylation at the *hTERT* promoter, and increase in *gluc* promoter activity, was evident with G4-disrupting mutations (Figure 2J-L and Figure 5C-E, Left and Right panel).

From loss of TRF2 binding at the G4-disrupted *hTERT* promoter we expected TL-dependent *hTERT* regulation to be affected. To test, TL was shortened in both -124G>A or -146 G>A mutated promoter-insert cell lines (Figure 5B; TRF2 protein levels Supplementary Figure 4A). Interestingly, TRF2 binding at the *hTERT* promoter with G4-disrupting mutations was not regained upon shortening of TL (Figure 5C Left and Right panel). This was in contrast to the increase in promoter TRF2 binding observed on TL shortening in case of the unmutated promoter (Figure 2J), supporting the role of G4s in *hTERT* promoter TRF2 binding and thereby in TL-dependent *hTERT* regulation. As expected, the difference in H3K27me3 deposition and *gluc* activity was not significant in -124G>A or -146G>A ST cells compared to the corresponding LT cells (Figure 5D, E Left and Right panel).

TRF2 R17 residue is required for repression of *hTERT* expression

To understand the role of TRF2 post translational modification(s) (PTM), if any, on *hTERT* repression we screened TRF2 mutants[36]. TRF2 mutants (arginine methylation deficient R17H[37]; acetylation deficient K176R, K190R[38] or phosphorylation deficient T188N[39] were expressed in HT1080 cells in a background where endogenous TRF2 was silenced (Supplementary Figure 5A-C). Re-expression of TRF2-wild type (WT) repressed *hTERT* as expected; R17H and K176R increased *hTERT*; T188N and K190R gave relatively moderate change (Supplementary Figure 5A-C). Noting that N-terminal domain of TRF2 (with the R17 residue) was shown to interact with G4 DNA[25,40], and also the core histone H3[41] we focussed on understanding the role of TRF2-R17 at the *hTERT* promoter.

Dox inducible TRF2-R17H or TRF2-WT stable lines were made with HT1080, HCT116 and MDAMB231 cells. Induction of TRF2-R17H gave significant upregulation of *hTERT*; whereas as expected TRF2-WT repressed *hTERT* in all the three cell lines (Figure 6A, Supplementary Figure 5D; dox dose-dependent induction shown in Supplementary Figure 5E). Increase in *hTERT* with TRF2-R17H expression in contrast to its reduction with TRF2-WT was also clear from *hTERT* FISH (Figure 6B).

To understand loss of function we looked closely at TRF2-R17H DNA binding at the *hTERT* promoter. Binding of FLAG tagged-TRF2-R17H on the *hTERT* promoter was

insignificant compared to the FLAG tagged-TRF2-WT in HT1080 cells (Figure 6C). As expected from the loss of TRF2-R17H binding, REST, EZH2 and H3K27me3 occupancy was significantly low on the *hTERT* promoter for TRF2-R17H compared to TRF2-WT (Figure 6D-F).

TRF2 promotes H3K27 trimethylation in vitro

For deeper understanding of the role of TRF2 in H3K27 trimethylation we used the *in vitro* histone H3 methyltransferase assay. Purified histone H3 along with the reconstituted PRC2 repressor complex was analysed in presence/absence of recombinant TRF2-WT or TRF2-R17H for methyltransferase activity (Figure 6G, Supplementary Figure 5F, G). H3K27 trimethylation in the presence of H3 and the PRC2 complex was first confirmed. Following this, treatment with purified TRF2-WT gave further increase in H3K27 trimethylation whereas TRF2-R17H did not lead to any significant increase, relative to respective controls (Figure 6G). Interestingly, together these support a direct function of TRF2 in histone H3K27 trimethylation in presence of the PRC2 complex, where the R17 residue of TRF2 plays a necessary role.

Discussion:

Here we show relatively long telomeres induce permissive chromatin at the *hTERT* promoter. Conversely, shorter telomeres give closed chromatin at the promoter. Resulting in telomere-dependent *hTERT* transcription in multiple cell types/models such as: short/long telomere HT1080, HCT116 and MDAMB231 cells; temporal TL elongation with subsequent shortening; TL-dependent transcription from artificially inserted *hTERT* promoter; including in tumour cells grown *in vivo* in mice. TRF2 binding at the *hTERT* promoter decreased/increased with TL elongation/shortening affecting TRF2-dependent recruitment of epigenetic modulators REST and the PRC2 repressor complex; resulting loss/gain in the repressor histone H3K27 trimethylation up or down regulated *hTERT* (Figure 7).

TRF2 binding outside telomeres, or non-telomeric TRF2, has been described earlier[16,42–44]. Here we demonstrate non-telomeric TRF2 binding to be dependent on

telomeres as proposed by the TSP model (Figure 1): Telomeric sequestering of TRF2, in case of longer telomeres, decreased non-telomeric binding; shorter telomeres conversely increased non-telomeric TRF2. We asked whether and how TSP affected *hTERT* regulation through non-telomeric TRF2 binding at the *hTERT* promoter.

An earlier paper showed long telomeres on the chromosome 5p interacted with the proximal *hTERT* locus (1.2 Mb away) by physical chromatin looping (TPE-OLD)[15]. Resulting heterochromatinization due to telomeric factors, including TRF2, repressed *hTERT*; loss of looping on telomere shortening de-repressed *hTERT*. We, on the other hand, observed long telomeres induce, and shorter TL repress *hTERT* transcription, suggesting this was distinct from looping-induced interactions. An important underlying difference about the nature of TRF2 at the *hTERT* promoter must be noted: in TPE-OLD, TRF2 is telomere-associated, whereas TRF2 is non-telomeric in TSP. To confirm non-telomeric TRF2 binding we reasoned in two ways. (a) Telomere-associated TRF2 is likely to be present with other telomeric factors like RAP1 and TRF1[17], and (b) inserted an *hTERT* promoter-reporter >40 Mb from telomeres where looping interaction was unlikely. While TRF2 binding at the *hTERT* promoter was clear, RAP1 or TRF1 was absent[21]. Furthermore, *hTERT* promoter activity from the inserted reporter was TL-dependent (Figure 2H-L). These support *hTERT* promoter-bound TRF2 as non-telomeric, and indicate the two models (TPE-OLD and TSP) are likely context-specific.

The overwhelming understanding, particularly in cancer cells, suggest *hTERT* activation drives telomere elongation/maintenance[3,8,11,45]. Here we tested the contrary, *i.e.*, if telomeres control *hTERT* expression? We engineered cells for increased TL, this upregulated *hTERT*. Multiple lines of evidence support causal role of telomeres in *hTERT* regulation. (a) Temporally induced TL elongation over days, using exogenous *hTERT*, activated the endogenous *hTERT* promoter gradually. As TL receded, after discontinuing induction, the endogenous *hTERT* promoter was re-suppressed (Figure 3). (b) TL elongation, by exogenous *hTERT*, or independent of *hTERT* (GTR oligonucleotides) in different cell types produced *hTERT* activation (Figure 2). (c) TL shortening, on the other hand, caused *hTERT* suppression (Figure 2). (d) Artificially introduced *hTERT* promoter reporter was activated following TL elongation (Figure 2 and 5). (e) And, finally, the underlying mechanisms involved *hTERT*-promoter TRF2

binding that was TL-dependent; TRF2-mediated recruitment of epigenetic factors closed/opened the promoter (Figure 2E-F, Figure 3D-E).

hTERT promoter G4s had a causal role in telomere-induced *hTERT* regulation. Promoter TRF2 binding is G4-dependent[21], therefore, as expected, TRF2-induced suppression of the *hTERT* promoter activity was lost when devoid of G4s (Figure 5). Interestingly, however, the *hTERT* promoter on G4 disruption also lost TL dependence (Figure 5). Together, this builds further support for a TL-driven mechanism of *hTERT* regulation.

The role of TRF2 in telomere protection stands well-established[46–48]. Here we describe the function of TRF2 in TL-dependent *hTERT* regulation. Long telomeres sequester more TRF2 for telomere protection, this reduces TRF2 at the *hTERT* promoter. Resulting de-repression of *hTERT*, and increased hTERT levels in turn synthesize (Figure 2) and help maintain longer telomeres (increased telomerase activity was evident, Supplementary figure 2B). The reversal of this was observed on TL shortening. Taken together, these suggest a feed-forward model that signals between telomeres and *hTERT* through TRF2. For this it was important that TRF2 levels are relatively unaltered as TL changes, which was the case (Supplementary Figure 1A). Multiple passaging of HCT116 cells (necessary for TL shortening with *hTERC* knockdown) leads to TRF2 depletion; reported to be p53-dependent. Therefore, p53-null HCT116 cells were used where TRF2 levels remained unchanged on multiple passaging (described in Methods, Supplementary Figure 1A) [49,50].

Although xenograft mice tumours indicate TL-induced *hTERT* activation might be active *in vivo*, results here are primarily from cells engineered for TL elongation/shortening (Figure 4). While these open new avenues additional work would be necessary to understand broader implications. For example, it is not clear how the initial TL elongation (which results in *hTERT* reactivation) is triggered during tumorigenic transformation. Interestingly, recent work shows telomere transfer from antigen presenting cells (APCs) result in telomere elongation of specific T cell populations, subsequent telomerase expression induced proliferative expansion during T cell activation[51]. This suggests the possibility of telomere transfer between tumour and immune/other cells within the tumour microenvironment might alter TL contributing to *hTERT* activation. In summary, our results reveal heretofore unknown

mechanisms of *hTERT* activation by telomeres. Together, these support a model that mechanistically connects telomeres to *hTERT* that might help improve understanding of telomere-related physiological events particularly tumorigenesis, ageing and de-differentiation[8,20,52–55].

Acknowledgements

The authors thank Balam Singh for management of laboratory and resources. We are thankful to all members of the S.C. laboratory for their suggestions/inputs and the IGIB Core Imaging Facility for its service facility. Research fellowships to A.S.G., S.V.M., D.S., R.D., J.J., S.D., A.K.M., S.S.R., S.S., A.K.B, D.K., A.S., S.S., S.B. (CSIR) and M.Y.(UGC) are acknowledged. S.C. acknowledges support from Wellcome Trust/DBT India Alliance Fellowship (IA/S/18/2/504021) for research grants. Support from Council of Scientific and Industrial Research (CSIR) and Department of Biotechnology (DBT) to S.C. are also acknowledged.

Author contributions

Conceptualization, S.C.; Methodology, A.S.G., S.V.M., D.S., R.D., J.J., S.D., A.K.M., M.Y., S.S.R., S.S., A.S.,S.S,R.K.M; Validation A.S.G.,S.V.M.,S.B.,A.S.,S.D.; Formal Analysis A.S.G.; Investigation, A.S.G., S.V.M., D.S., R.D., J.J., S.D., A.K.M., M.Y.A.K.B.; Resources A.S.G.,A.S.,S.S,R.K.M, A.S.,D.K.,S.B.; Data Curation, A.S.G.; Writing – Original Draft Preparation, A.S.G; Writing – Review & Editing, S.C. and A.S.G.; Visualization, A.S.G.; Supervision, S.C.; Project Administration, A.S.G., S.C.; Funding Acquisition S.C.

Declaration of interests

None

Inclusion and diversity statement

The authors support diverse, inclusive and equitable conduct of research

Methods

EXPERIMENTAL MODEL AND SUBJECT DETAILS

Source and maintenance details of all cell lines used in the study

Cancer cell lines

HT1080 (obtained from ATCC) and its derivative cell line HT1080-LT were maintained in Minimum Eagle's Essential Medium (MEM) (Sigma-Aldrich) with 10% Fetal Bovine Serum (FBS) (Gibco). HCT116 WT (gift from Prof. Vinay Tergaonkar's lab), HCT116 p53 null (gift from Prof. Bert Vogelstein's lab), MDAMB 231 (gift from Mayo Clinic, Minnesota, USA) along with their derivative cells (short or long telomeres) and HEK293T (purchased from NCCS, Pune) CRISPR CCR5 locus insert cell lines were grown in Dulbecco's Modified Essential Medium High Glucose (DMEM-high Glucose) (Sigma-Aldrich) with 10% FBS. Doxycycline (dox) Inducible TRF2 cells in HT1080 and Dox-HT1080 were cultured in MEM and dox Inducible TRF2 HCT116 and MDAMB231 and Dox-MDAMB 231 cells were cultured in DMEM-High Glucose, all supplemented with 10% tetracycline-free Fetal Bovine Serum (FBS) (Clontech and DSS Takara). Cells were trypsinized and sub-cultured in desired culture vessels when at 90% confluency. All cells were grown in 5% CO2, 95% relative humidity and 37°C culturing conditions.

Generation of short or long TL cellular model systems

1. A longer telomere version of **HT1080** fibrosarcoma cells (termed super-telomerase and referred to as HT1080-LT in the current paper) was generated by overexpression of telomerase (hTERT) and telomerase RNA component (*hTERC*). It was received as a generous gift from Lingner lab[22].
2. **HCT116 p53 null** or knockout cells were used as parent cell line to generate a short telomere version using commercial *hTERC* knockdown plasmid and a scrambled control from Santa Cruz Biotechnology. Over multiple passaging under puromycin selection, telomere length reduction was achieved. This HCT116 ST/LT cell line pair was generated under p53 knockout (p53$^{-/-}$) background to prevent p53 regulated *Siah1* mediated TRF2 degradation and ensure similar TRF2 protein levels[49,50].

3. A long telomere length version of the **MDAMB231** cell line was generated using the alternative lengthening of telomeres (ALT) mechanism[23]. Cells were treated with GTR (guanine-rich terminal repeats) oligos at 3uM concentration, in serum-free media for 24h. Post treatment, the cells were kept in DMEM- High Glucose for 24 hrs. Sequential treatment for 6 feedings (i.e., 12 days), resulted in the increase in telomere length by 4 folds as determined by Telomeric PNA-Flow cytometry (FACS).
4. **HCT116** cells were utilised to generate a short telomere length version by means of CRISPR-Cas9 based telomere trimming. A telomeric sequence specific sgRNA (tel-sgRNA) and *Sp*Cas9 expressing plasmid was transfected in the cells to generate a telomere shortened version of the cells. This mode of telomere shortening is quicker than that via *hTERC* knockdown (as in point 2). Telomere length was quantified by FACS after 3 days after transfection- post puromycin treatment to select out transfected cells (with shorter telomeres). Telomeric sgRNA: GTTAGGGTTAGGGTTAGGGTTA
5. To generate the TL elongation and shortening model **Dox-HT1080** using the doxycycline inducible hTERT expression system, (stable cell generation discussed below), the cells were treated with 1µg/mL Dox daily for ten days. Beyond Day-10, cells were maintained with or without Dox treatment till Day-16 and telomere length measured. Since no further telomere elongation beyond Day-10 was observed, the cells were cultured till Day24 without dox treatment to represent telomere shortening model. Similar treatment was carried out for **Dox-MDAMB231 system**- dox treatment was discontinued after Day-10 and experiments performed till Day 14.
6. 1300 bp region of *hTERT* promoter starting from 48 bp downstream of TSS with **Gaussia Luciferase reporter** was procured from Genecopoeia-HPRM25711-PG04 (pEZX-PG04.1 vector) and inserted in **HEK293T** cells via CRISPR-Cas9 technology as discussed in[21]. The telomeric sequence specific sgRNA (tel-sgRNA) and *Sp*Cas9 expressing plasmid as mentioned for HCT116, these CRISPR modified cells were transfected to generate a telomere shortened version of the CRISPR cells for both unmutated *hTERT* promoter and G-quadruplex (G4) disrupting mutant promoter forms, namely -124G>A and -146G>A. Telomere length was quantified by FACS, after 3 days of transfection

post puromycin treatment to select out transfected cells (with shorter telomeres).

Doxycycline (dox) inducible hTERT and TRF2 PTM Lentiviral stable cell generation

Doxycycline (dox) inducible hTERT construct and TRF2 WT and R17H PTM variant construct- both in pCW57.1 backbone were individually transfected with 3rd generation lentiviral packaging plasmids (pRRE, pREV and pMD2.G) in 4:3:3:2 ratio in HEK293 Lenti-X cells for viral particle generation. 12h post transfection, media change was given and incubated in general culture conditions for 72h. Viral particles were then collected by filtering the media with 0.45 µM syringe filter. This viral particle filtrate was then added along with fresh media and Polybrene (5µg/mL) to HT1080 and MDAMB231 cells (for ind. hTERT construct) and HT1080, HCT116 WT cells and MDAMB231 cells (for ind. TRF2 variant construct); incubated for 24h. Post 24h, media containing viral particle was safely discarded and fresh media added. Next, puromycin selection was given to the cells until transduced population of cells could be stably maintained.

Generation of TRF2 Post translational modification variants via Site directed mutagenesis

The TRF2 post translational modification variants were generated using site-directed mutagenesis by PCR method. The primers containing required mutation (as documented in table) were used to amplify the entire plasmid containing WT TRF2 sequence. The PCR product was purified and transformed into DH5*a* E. coli cells. Then the mutated plasmid constructs were isolated and confirmed by sangar sequencing.

Mutation	Foreward primer (5'-3')	Reverse primer (5'-3')
K190R	ccaaggaccccacaactcagaggctgagaaatga	tcatttctcagcctctgagttgtggggtccttgg
T188N	Tgtccaaggaccccacaaatcagaagctgagaaat	atttctcagcttctgatttgtggggtccttggaca

K176R	aaaaacaaagaatttgaaaaggcttcaagaattttgaaaaacatatgtccaaggac	gtccttggacatatgtttttcaaaattcttgaagccttttcaaattctttgttttt
R17H	cgggcagctggccaccgggcgtcccgc	gcgggacgcccggtggccagctgcccg

Generation of Xenograft tumour in NOD-SCID mice:

Tumour xenograft generation in NOD SCID mice was outsourced to Vivo Bio TechLtd – Telangana, India. 2.5 million cells of HT1080, HT1080-LT each were injected subcutaneously in healthy male mice (4-6 weeks old) and monitored for tumour growth. Tumours were harvested by sacrificing mice when tumour growth reached an average volume of 600 mm3(± 100).

Telomere length determination

Telomere length was determined using two methods - RT-PCR based and Flow Cytometry based. For flow cytometry-based evaluation using Agilent DAKO kit, 2 x10^6 cells were divided in two fractions- for FITC labelled Telomeric PNA probe (Agilent DAKO kit) and unlabelled control cells. The cells fractions were washed, further labelled with PI for whole DNA content as per manufacturer's protocol and fluorescence signal acquired for at least 20,000 events on BD Accuri C6 flow cytometer. FCS files were then analysed using FlowJo version 10.8.1 software. Fold change of telomere length relative to reference cell samples was calculated using Median Fluorescence signal intensity values of labelled and unlabelled sample preparations according to kit provided formula.

For RT-PCR based telomere length estimation, genomic DNA was isolated using the Wizard Genomic DNA Purification kit. At least 2 dilutions of genomic DNA in the range of 10ng- 60ng were prepared for each sample and qRT-PCR was setup for telomere specific primers and single copy gene 36B4 specific primer from O'Callaghan et al., 2008 and Cawthon et al 2002 respectively[56,57]. Ct value of telomeric primer was compared to respective sample 36B4 and then fold change over control sample was calculated.

The primers used are:

Tel F CGGTTTGTTTGGGTTTGGGTTTGGGTTTGGGTTTGGGTT

Tel R GGCTTGCCTTACCCTTACCCTTACCCTTACCCTTACCCT

36B4F CAGCAAGTGGGAAGGTGTAATCC

36B4R CCCATTCTATCATCAACGGGTACAA

Telomerase activity using ELISA TRAP

ELISA TRAP was performed as described in Sharma et al 2021. Briefly, $1x10^6$ cells were lysed using mild lysis buffer CHAPS supplemented with RNase inhibitor to prevent loss of enzymatic activity (due to *hTERC* degradation) and PIC to prevent protein degradation. Protein concentration in the lysate was estimated and diluted accordingly to a concentration of 0.5 µg/µL. 2µg of protein was then used to set up telomerase repeat amplification protocol (TRAP) PCR[58]. This was performed using PCR master mix provided with ROCHE TeloTAGGG Telomerase PCR ELISA kit which uses 3' biotinylated telomeric sequence repeat primers, P1-TS primers. Telomerase from the lysate extends the P1-TS primer which in next step acts as template for amplicon generation using P1-TS primer and (TTAGGG)6 repetitive sequences- P2. After this PCR, dioxygenin (dig) tagged telomere specific detection probe are hybridised to denatured PCR products. These tagged biotinylated PCR products are then bound to streptavidin coated plates and quantified using anti-dig-Peroxidase conjugated antibody, which produces coloured product upon metabolizing substrate, TMB).

ChIP (chromatin immunoprecipitation)

Relevant Primary antibodies (TRF2 Novus Biologicals #NB110-57130, REST Sigma Aldrich #17-641, EZH2 Cell Signal Technology # 5246, H3K27me3 Abcam #ab6002, H3 Abcam # ab1791, FLAG Merck #F3165) and suitable IgG (from Millipore, for Isotype control or Mock) were used to perform the ChIP assays as per protocol reported in Mukherjee et al. (2018)[17]. Briefly, 3 x 10^6 cells were harvested and fixed with 1% formaldehyde for 10min. Post washing with ice cold PBS, the fixed cells were lysed in SDS based lysis buffer with 2X mammalian Protease Inhibitor Cocktail and subjected to chromatin fragmentation to an average size range of 200-300bp using Bioruptor (Diagenode). 10% fragmented chromatin was processed as Input fraction via Phenol-Chloroform- Isoamyl Alcohol (PCI) and Ethanol precipitation. Assay was performed with 3 µg of respective primary antibody incubated overnight on rotor at 4°C followed by immune complex pulldown with salmon sperm DNA saturated Protein G

Magnetic Dyna Beads. Subsequent washes with low salt, high salt and then LiCl buffers were performed and beads resuspended in TE (Tris-EDTA pH 8) for proteinase K treatment at 55°C, 2h. Thereafter, PCI was used to phase - separate DNA in aqueous layer; separated fraction was incubated with equal volumes of isopropanol, 3M sodium acetate and glycogen overnight at -20°C. Pulldown DNA was then precipitated by centrifugation and pellet washed in 70% ethanol before air drying and resuspending in nuclease free water. Chromatin pulldown was validated by q-PCR analysis.

Analysis of ChIP experiments

ChIP-q-PCR for TRF2, REST and EZH2 chromatin pulldowns was performed with equal amount of DNA for each fraction, determined by Qubit HS DNA kit. Then, fold change was calculated over IgG (Mock) by using average Ct values. In case of histone ChIP assays too, equal amount of DNA from each histone ChIP and its respective total H3 were used in qPCR. Ct values for Histone mark and total H3 were normalized to 1% Input and thereafter fold change over total H3 was calculated.

Transfections

Cells were seeded a day before transfection at 70% confluency in a 6 well plate. 1.5µg plasmid per well was transfected by complexing with FUGENE at 1:3 (DNA: Reagent) ratio following manufacturer's protocol.12h post transfection media change was given to the cells and later harvested for mRNA and protein analysis after 36h of media change.

Real time PCR for mRNA expression

Total RNA isolation was performed using TRIzol Reagent (Invitrogen, Life Technologies) as per manufacturer's instructions. RNA quantification and cDNA preparation was done using Applied Biosciences kit. Quantitative real-time PCR using SYBR Green based method (DSS TAKARA) was employed to estimate relative transcript levels of mRNAs with GAPDH as housekeeping control gene for internal normalization. Average fold change was calculated by difference in internally normalised threshold cycles (Ct) between test and control samples. All experiments were performed in three biological replicates; with technical triplicates of each primer pair and sample combination for q-PCR analysis.

In HT1080 ST/LT, Dox-HT1080 and Dox-MDAMB231 cells with overexpression of hTERT and *hTERC* (for HT1080-LT), primer pair specific for *hTERT* mRNA 3'UTR was implemented to capture the status of endogenous *hTERT* expression in addition to standard primers spanning exon 15/16 (full length) and exon 7/8 (active reverse transcriptase) forms. 3'UTR *hTERT* primers were designed with help from UTRdb 2.0.

mRNA primers:

hTERT 3' UTR Fwd: AATTTGGAGTGACCAAAGGTGT
hTERT 3' UTR Rev: TATTTTACTCCCACAGCACCTC
GAPDH FP TGCACCACCAACTGCTTAGC
GAPDH RP GGCATGGACTGTGGTCATGAG
TRF2 FP CAGTGTCTGTCGCGGATTGAA
TRF2 RP CATTGATAGCTGATTCCAGTGGT
18S FP TTCGGAACTGAGGCCATGAT
18S RP TTTCGCTCTGGTCCGTCTTG

hTERT mRNA FISH

Untreated or transfected cells were seeded on coverslip for this experiment and processed according to Stellaris RNA FISH protocol. Briefly, cells were fixed with fixation buffer for 10min at RT. This was followed by PBS wash and permeabilization with 70% (v/v) ethanol. For Hybridization, 125nM of probe per 100ul of Hybridization buffer was mixed and added on to parafilm surface in a humidified chamber. Coverslips were then placed on this drop with cells side down (post wash in wash buffer A containing formamide), incubated in dark at 37°C overnight. After incubation, the coverslips were transferred to fresh 1ml Wash Buffer A for 30min. This was followed by nuclear staining with DAPI in the same buffer, in the dark for 30min maximum. Finally, coverslip was washed in Wash Buffer B for 5min and then mounted on slide with anti-fade mounting reagent.

Western blotting

For checking protein levels, cells were harvested, PBS wash given and lysate prepared with RIPA with 1x mammalian PIC. Proteins were resolved using 10% SDS-PAGE and transferred on polyvinylidene difluoride (PVDF) membranes (Biorad).

Membranes were blocked with 5% skimmed milk and then probed suitably with primary antibodies- anti-TRF2 antibody (Novus Biological), anti-TERT antibody (Abcam), anti-REST(Millipore), anti-EZH2(CST) and anti-GAPDH antibody (Santa-cruz). Anti-mouse and anti-rabbit HRP conjugated secondary antibodies were from CST. Blots were developed using BioRad ClarityMax HRP chemiluminescence detection kit and images acquired on LAS500 GE ChemiDoc system.

Gaussia-luciferase assay

Secreted Gaussia luciferase signal in the CRISPR modified short telomere and control cells (WT, -124G>A and -146G>A -ST/LT) was quantified using Promega Gaussia luciferase kit according to manufacturer's protocol. Luminescence signal was normalised to total protein for each condition.

Quantification and statistical analysis

Each experiment was performed in at least three biological replicates. Average of biological replicates was calculated and error bars represent ± standard deviations from mean values; p values were then calculated. Comparison between two conditions (control and TRF2 overexpressed, for example) was evaluated using paired/ unpaired Student's T-test. For multivariate comparison two-way ANOVA and for datasets with N> 5, Mann Whitney U test was performed (*$p < 0.05$, **$p < 0.01$, ***$p < 0.005$, ****$p < 0.0001$). All calculations and graph plotting were done with GraphPad Prism V8.0.2.

References

1. Rhodes, D., Fairall, L., Simonsson, T., Court, R. & Chapman, L. *Telomere architecture*. *EMBO reports* vol. 3 (2002).

2. O'Sullivan, R. J. & Karlseder, J. Telomeres: protecting chromosomes against genome instability. *Nat Rev Mol Cell Biol* **11**, 171–181 (2010).

3. Shay, J. W. & Wright, W. E. Telomeres and telomerase: three decades of progress. *Nat Rev Genet* 1(2):88-96 (2019) doi:10.1038/s41576-019-0099-1.

4. Greider, C. W. & Blackburn, E. H. Identification of a specific telomere terminal transferase activity in tetrahymena extracts. *Cell* **43**, 405–413 (1985).

5. Blackburn, E. H. Switching and Signaling at the Telomere. *Cell* **106**, 661–673 (2001).

6. Autexier, C. & Lue, N. F. The Structure and Function of Telomerase Reverse Transcriptase. *Annu Rev Biochem* **75**, 493–517 (2006).

7. Shay, J. W. & Bacchetti, S. A survey of telomerase activity in human cancer. *Eur J Cancer* **33**, 787–791 (1997).

8. Artandi, S. E. & DePinho, R. A. Telomeres and telomerase in cancer. *Carcinogenesis* **31**, 9–18 (2010).

9. Pandita, R. K. *et al.* Single-Strand DNA-Binding Protein SSB1 Facilitates TERT Recruitment to Telomeres and Maintains Telomere G-Overhangs. *Cancer Res* **75**, 858–869 (2015).

10. Heaphy, C. M. *et al.* Prevalence of the Alternative Lengthening of Telomeres Telomere Maintenance Mechanism in Human Cancer Subtypes. *Am J Pathol* **179**, 1608–1615 (2011).

11. Roake, C. M. & Artandi, S. E. Regulation of human telomerase in homeostasis and disease. *Nat Rev Mol Cell Biol* **21**, 384–397 (2020).

12. Sarthy, J. F. & Baumann, P. Apollo—Taking the Lead in Telomere Protection. *Mol Cell* **39**, 489–491 (2010).

13. Souza, Y. D., Lauzon, C., Chu, T. W. & Autexier, C. Regulation of telomere length and homeostasis by telomerase enzyme processivity. 676–687 (2012) doi:10.1242/jcs.119297.

14. Robin, J. D. *et al.* Telomere position effect: Regulation of gene expression with progressive telomere shortening over long distances. *Genes Dev* (2014) doi:10.1101/gad.251041.114.

15. Kim, W., Ludlow, A. T., Min, J. & Robin, J. D. Regulation of the Human Telomerase Gene TERT by Telomere Position Effect-Over Long Distances (TPE- OLD): Implications for Aging and Cancer. (2016).

16. Mukherjee, A. K. *et al.* Telomere repeat–binding factor 2 binds extensively to extra-telomeric G-quadruplexes and regulates the epigenetic status of several gene promoters. *Journal of Biological Chemistry* 294(47):17709-17722. (2019) doi:10.1074/jbc.ra119.008687.

17. Mukherjee, A. K. *et al.* Telomere length-dependent transcription and epigenetic modifications in promoters remote from telomere ends. *PLoS Genet* **14**, (2018).

18. Mukherjee, A. K., Sharma, S. & Chowdhury, S. Non-duplex G-Quadruplex Structures Emerge as Mediators of Epigenetic Modifications. *Trends in Genetics* **xx**, 1–16 (2018).

19. Okamoto, K. & Seimiya, H. From the wings to the center stage of chromosomes. *Journal of Biological Chemistry* **294**, 17723–17724 (2019).

20. Vinayagamurthy, S., Ganguly, A. & Chowdhury, S. Extra-telomeric impact of telomeres: Emerging molecular connections in pluripotency or stemness. *Journal of Biological Chemistry* **295**, 10245–10254 (2020).

21. Sharma, S. *et al.* Human telomerase is directly regulated by non-telomeric TRF2-G-quadruplex interaction. *Cell Rep* **35**, 109154 (2021).

22. Cristofari, G. & Lingner, J. Telomere length homeostasis requires that telomerase levels are limiting. *EMBO J* **25**, 565–574 (2006).

23. Wright, W. E., Brasiskyte, D., Piatyszek, M. A. & Shay, J. W. Experimental elongation of telomeres extends the lifespan of immortal x normal cell hybrids. *EMBO J* **15**, 1734–41 (1996).

24. Myung, K. *et al.* Regulation of Telomere Length and Suppression of Genomic Instability in Human Somatic Cells by Ku86. *Mol Cell Biol* **24**, 5050–5059 (2004).

25. Bryan, T. M. & Baumann, P. G-Quadruplexes: From Guanine Gels to Chemotherapeutics. *Mol Biotechnol* **49**, 198–208 (2011).

26. Rawal, P. *et al.* Genome-wide prediction of G4 DNA as regulatory motifs: role in Escherichia coli global regulation. *Genome Res* **16**, 644–655 (2006).

27. Huppert, J. L. & Balasubramanian, S. G-quadruplexes in promoters throughout the human genome. *Nucleic Acids Res* **35**, 406–413 (2007).

28. Verma, A. *et al.* Genome-wide computational and expression analyses reveal G-quadruplex DNA motifs as conserved cis-regulatory elements in human and related species. *J Med Chem* **51**, 5641–5649 (2008).

29. Verma, A., Yadav, V. K., Basundra, R., Kumar, A. & Chowdhury, S. Evidence of genome-wide G4 DNA-mediated gene expression in human cancer cells. *Nucleic Acids Res* 37(13):4194-204 (2009) doi:10.1093/nar/gkn1076.

30. Palumbo, S. L., Ebbinghaus, S. W. & Hurley, L. H. Formation of a unique end-to-end stacked pair of G-quadruplexes in the hTERT core promoter with implications for inhibition of telomerase by G-quadruplex-interactive ligands. *J Am Chem Soc* **131**, 10878–10891 (2009).

31. Lim, K. W. *et al.* Coexistence of Two Distinct G-Quadruplex Conformations in the hTERT Promoter. *J Am Chem Soc* **132**, 12331–12342 (2010).

32. Huang, F. W. *et al.* Highly recurrent TERT promoter mutations in human melanoma. *Science (1979)* (2013) doi:10.1126/science.1229259.

33. Horn, S. *et al.* TERT promoter mutations in familial and sporadic melanoma. *Science (1979)* (2013) doi:10.1126/science.1230062.

34. Killela, P. J. *et al.* TERT promoter mutations occur frequently in gliomas and a subset of tumors derived from cells with low rates of self-renewal. *Proceedings of the National Academy of Sciences* **110**, 6021–6026 (2013).

35. Kang, H.-J. *et al.* A Pharmacological Chaperone Molecule Induces Cancer Cell Death by Restoring Tertiary DNA Structures in Mutant hTERT Promoters. *J Am Chem Soc* **138**, 13673–13692 (2016).

36. Walker, J. R. & Zhu, X.-D. Post-translational modifications of TRF1 and TRF2 and their roles in telomere maintenance. *Mech Ageing Dev* **133**, 421–434 (2012).

37. Mitchell, T. R. H., Glenfield, K., Jeyanthan, K. & Zhu, X.-D. Arginine Methylation Regulates Telomere Length and Stability. *Mol Cell Biol* **29**, 4918–4934 (2009).

38. Rizzo, A. *et al.* SIRT6 interacts with TRF2 and promotes its degradation in response to DNA damage. *Nucleic Acids Res* **45**, 1820–1834 (2017).

39. Tanaka, H. *et al.* DNA damage-induced phosphorylation of the human telomere-associated protein TRF2. *Proceedings of the National Academy of Sciences* **102**, 15539–15544 (2005).

40. Pedroso, I. M., Hayward, W. & Fletcher, T. M. The effect of the TRF2 N-terminal and TRFH regions on telomeric G-quadruplex structures. *Nucleic Acids Res* **37**, 1541–1554 (2009).

41. Konishi, A., Izumi, T. & Shimizu, S. TRF2 Protein Interacts with Core Histones to Stabilize Chromosome Ends. *Journal of Biological Chemistry* **291**, 20798–20810 (2016).

42. El Maï, M. *et al.* The telomeric protein TRF2 regulates angiogenesis by binding and activating the PDGFRβ promoter. *Cell Rep* (2014) doi:10.1016/j.celrep.2014.09.038.

43. Hussain, T. *et al.* Transcription regulation of CDKN1A (p21/CIP1/WAF1) by TRF2 is epigenetically controlled through the REST repressor complex. *Sci Rep* **7**, 11541 (2017).

44. Purohit, G., Mukherjee, A. K., Sharma, S. & Chowdhury, S. Extratelomeric Binding of the Telomere Binding Protein TRF2 at the PCGF3 Promoter Is G-Quadruplex Motif-Dependent. *Biochemistry* (2018) doi:10.1021/acs.biochem.8b00019.

45. Smogorzewska, A. & de Lange, T. Regulation of Telomerase by Telomeric Proteins. *Annu Rev Biochem* **73**, 177–208 (2004).

46. Sfeir, A. & de Lange, T. Removal of shelterin reveals the telomere end-protection problem. *Science* **336**, 593–597 (2012).

47. Schmutz, I., Timashev, L., Xie, W., Patel, D. J. & de Lange, T. TRF2 binds branched DNA to safeguard telomere integrity. *Nat Struct Mol Biol* **24**, 734–742 (2017).

48. van Steensel, B., Smogorzewska, A. & de Lange, T. TRF2 Protects Human Telomeres from End-to-End Fusions. *Cell* **92**, 401–413 (1998).

49. Sur, S. *et al.* A panel of isogenic human cancer cells suggests a therapeutic approach for cancers with inactivated p53. *Proceedings of the National Academy of Sciences* **106**, 3964–3969 (2009).

50. Fujita, K. *et al.* Positive feedback between p53 and TRF2 during telomere-damage signalling and cellular senescence. *Nat Cell Biol* **12**, 1205–1212 (2010).

51. Lanna, A. *et al.* An intercellular transfer of telomeres rescues T cells from senescence and promotes long-term immunological memory. *Nat Cell Biol* **24**, 1461–1474 (2022).

52. Wong, J. M. & Collins, K. Telomere maintenance and disease. *The Lancet* **362**, 983–988 (2003).

53. Muñoz, P., Blanco, R. & Blasco, M. A. Role of the TRF2 telomeric protein in cancer and ageing. *Cell Cycle* vol. 5 718–721 Preprint at https://doi.org/10.4161/cc.5.7.2636 (2006).

54. Jafri, M. A., Ansari, S. A., Alqahtani, M. H. & Shay, J. W. Roles of telomeres and telomerase in cancer, and advances in telomerase-targeted therapies. *Genome Med* **8**, (2016).

55. Rossiello, F., Jurk, D., Passos, J. F. & d'Adda di Fagagna, F. Telomere dysfunction in ageing and age-related diseases. *Nat Cell Biol* **24**, 135–147 (2022).

56. Cawthon, R. M. *Telomere measurement by quantitative PCR*. *Nucleic Acids Research* vol. 30 (2002).

57. O'Callaghan, N. J., Dhillon, V. S., Thomas, P. & Fenech, M. A quantitative real-time PCR method for absolute telomere length. *Biotechniques* **44**, 807–809 (2008).

58. Kim, N. W. *et al.* Specific association of human telomerase activity with immortal cells and cancer. *Science* **266**, 2011–2015 (1994).

Figure 1.

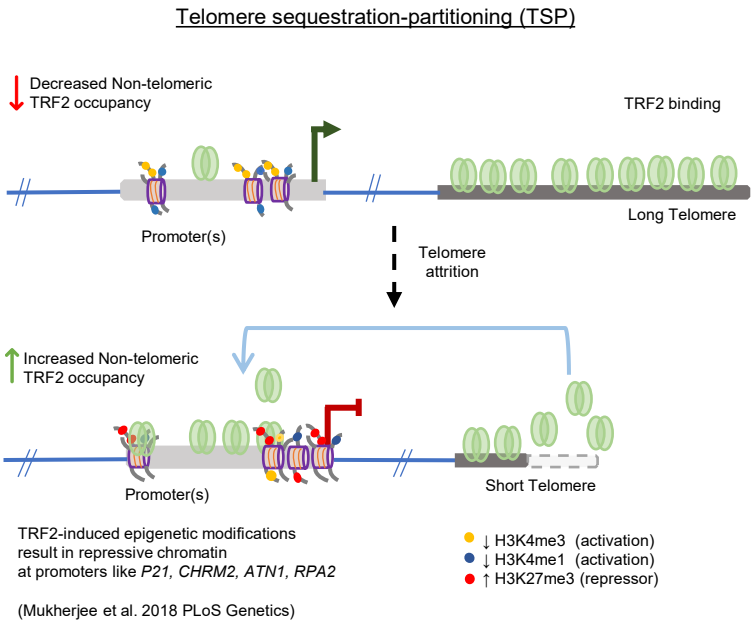

Figure 1. Graphical representation of the Telomere Sequestration Partitioning (TSP) model.

The binding of TRF2 outside of telomeric regions (non-telomeric) is dependent on telomere length. When telomeres shorten, the presence of TRF2 at telomeres diminishes, resulting in increased TRF2 binding at non-telomeric sites. This shift in TRF2 distribution triggers epigenetic modifications at promoters showing telomere-dependent gene regulation.

Figure 2.

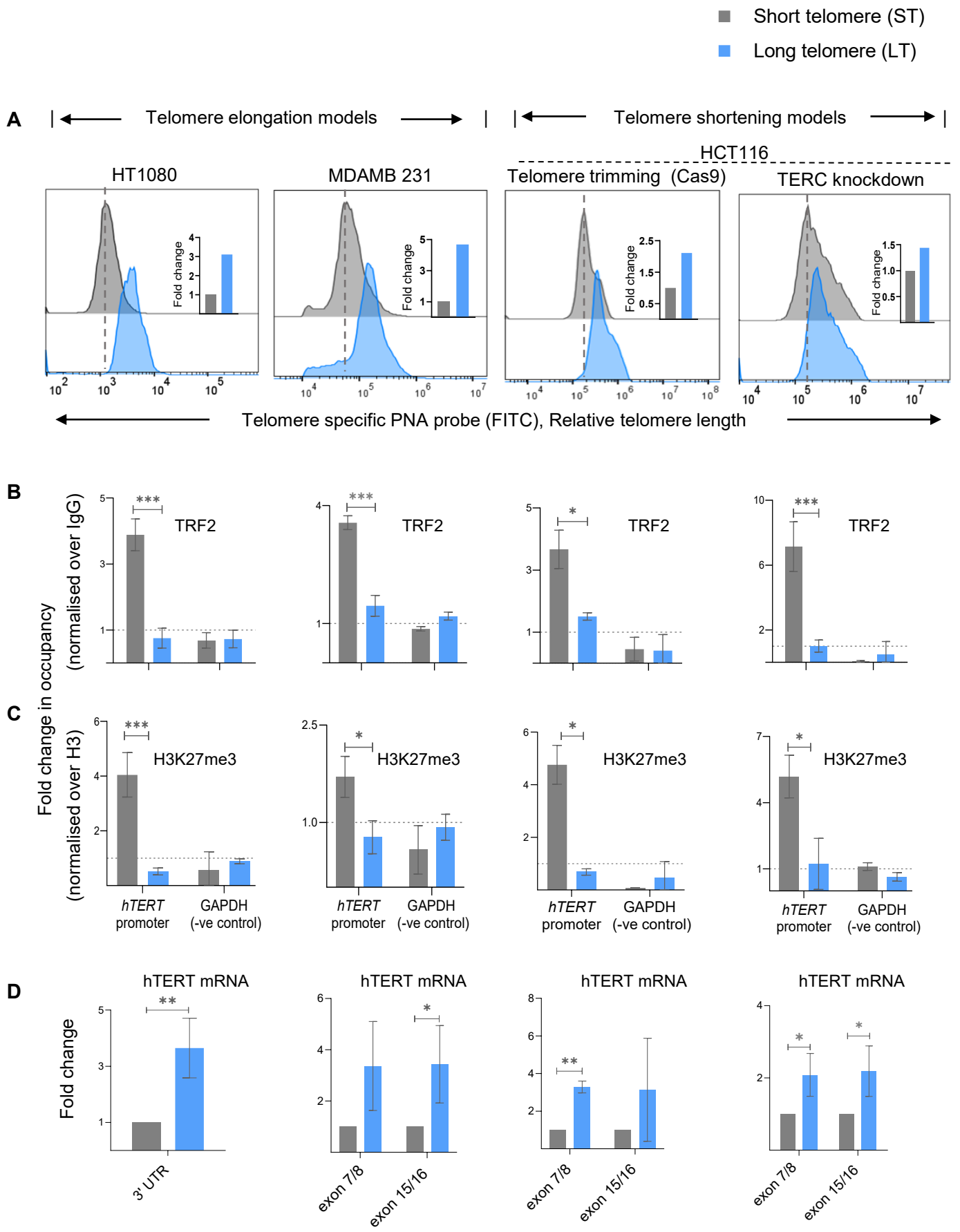
Short telomere (ST)
Long telomere (LT)
A
Telomere elongation models
Telomere shortening models
HCT116
HT1080
MDAMB 231
Telomere trimming (Cas9)
TERC knockdown
Fold change
Telomere specific PNA probe (FITC), Relative telomere length
B
Fold change in occupancy (normalised over IgG)
TRF2
C
(normalised over H3)
H3K27me3
hTERT promoter
GAPDH (-ve control)
D
Fold change
hTERT mRNA
3' UTR
exon 7/8
exon 15/16

Figure 2.

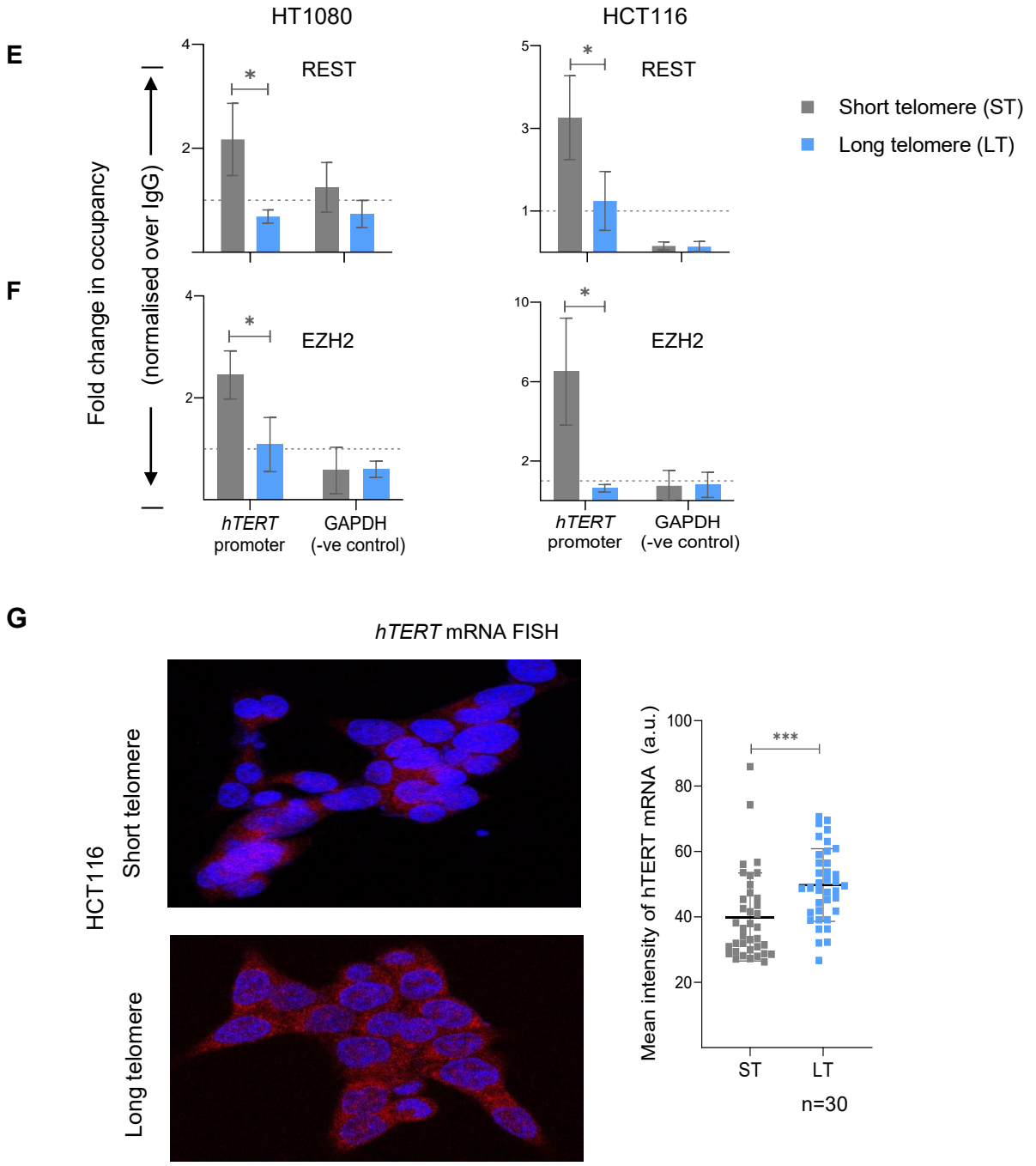
E
F
G
HT1080
HCT116
REST
EZH2
Fold change in occupancy
(normalised over IgG)
Short telomere (ST)
Long telomere (LT)
hTERT promoter
GAPDH (-ve control)
hTERT mRNA FISH
HCT116
Short telomere
Long telomere
Mean intensity of hTERT mRNA (a.u.)
ST
LT
n=30

Figure 2.

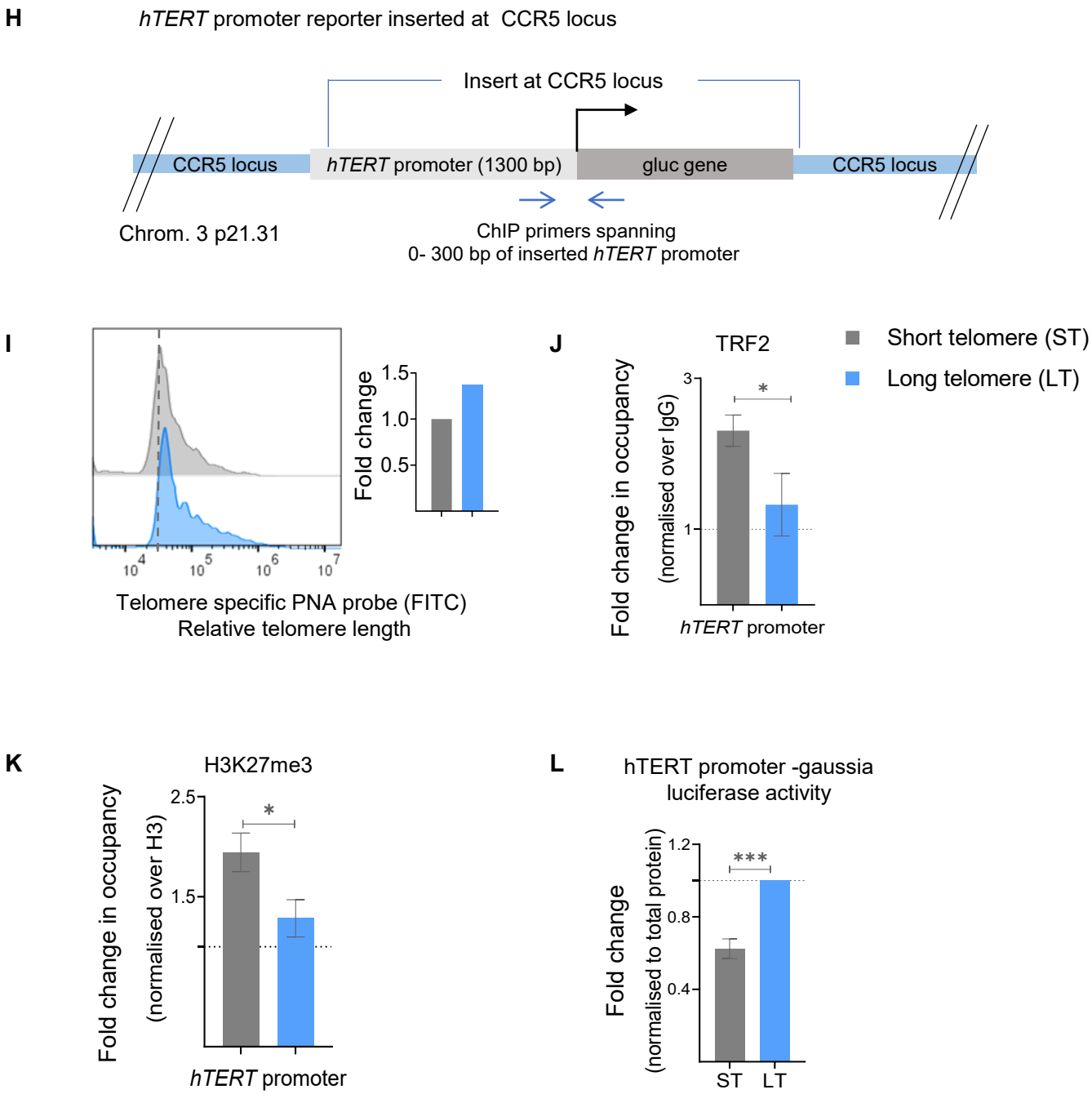

Figure 2. Telomere dependent non-telomeric TRF2 binding at the *hTERT* promoter controls *hTERT* expression

(A) Telomere length in isogenic cancer cell lines with short telomeres (ST, in grey) or long telomeres (LT, in blue) namely, HT1080- ST/LT, MDAMB 231-ST/LT, and HCT116-ST/LT (Telomere trimming-Cas9 and *hTERC* knockdown) as determined by Flow cytometry (FACS). MDAMB 231-ST/LT and HCT116-ST/LT Telomere trimming-Cas9 models were generated by telomerase independent mode of TL alteration (See Methods). Relative fold change shown in insets with FACS plots.

(B-C) ChIP followed by qRT-PCR at the 0-300 bp *hTERT* promoter (upstream of TSS) for TRF2 (B) and H3K27me3 (C) in respective ST/LT cells; occupancy normalized to respective IgG or total Histone H3 (for H3K27me3). qPCR on *GAPDH* promoter used as negative control in all cases.

(D) *hTERT* mRNA expression by qRT-PCR in above-mentioned ST/LT cells normalized to *GAPDH* or 18S mRNA levels. Primers specific to 3'UTR for endogenous *hTERT* was used for HT1080-ST/LT system where telomerase was overexpressed for telomere elongation; primers for functional (reverse transcriptase domain) (exon7/8) and full length (exon 15/16) transcript were used for all other systems.

(E, F) ChIP followed by qRT-PCR at the *hTERT* promoter for REST (E) and EZH2 (F) in HT1080-ST/LT (left panel) and HCT116-ST/LT (*hTERC* knockdown) (right panel); occupancy normalized to respective IgG. qPCR on *GAPDH* promoter used as negative control in all cases.

(G) *hTERT* mRNA FISH signal (red) with DAPI (blue) and quantification (right panel) in HCT116-ST/LT (*hTERC* knockdown), n=30;

(H) Scheme depicting CRISPR modified HEK293T cells with 1300 bp *hTERT* promoter driving gaussia luciferase (gluc) construct inserted at the CCR5 safe harbor locus. Scheme denotes ChIP primers used to study chromatin occupancy of 0-300 bp *hTERT* promoter region inserted at the exogenous locus

(I) Relative fold change in telomere length in *hTERT* promoter insert cells following telomere shortening determined by FACS; quantification in right panel.

(J, K) ChIP followed by qRT-PCR at the insert 0-300 bp *hTERT* promoter (upstream of TSS) for TRF2 (J), and H3K27me3 (K) in ST/LT cells. Occupancy normalized to respective IgG or total histone H3 (for H3K27me3)

(L) *hTERT* promoter-gaussia luciferase activity in ST cells over LT cells from inserted exogenous with *hTERT* promoter. Reporter activity normalized to respective total protein levels.

Error bars represent ± SDs from mean. p values are calculated by paired/unpaired t test (*$p < 0.05$, **$p < 0.01$, ***$p < 0.005$, ****$p < 0.0001$)

Figure 3.

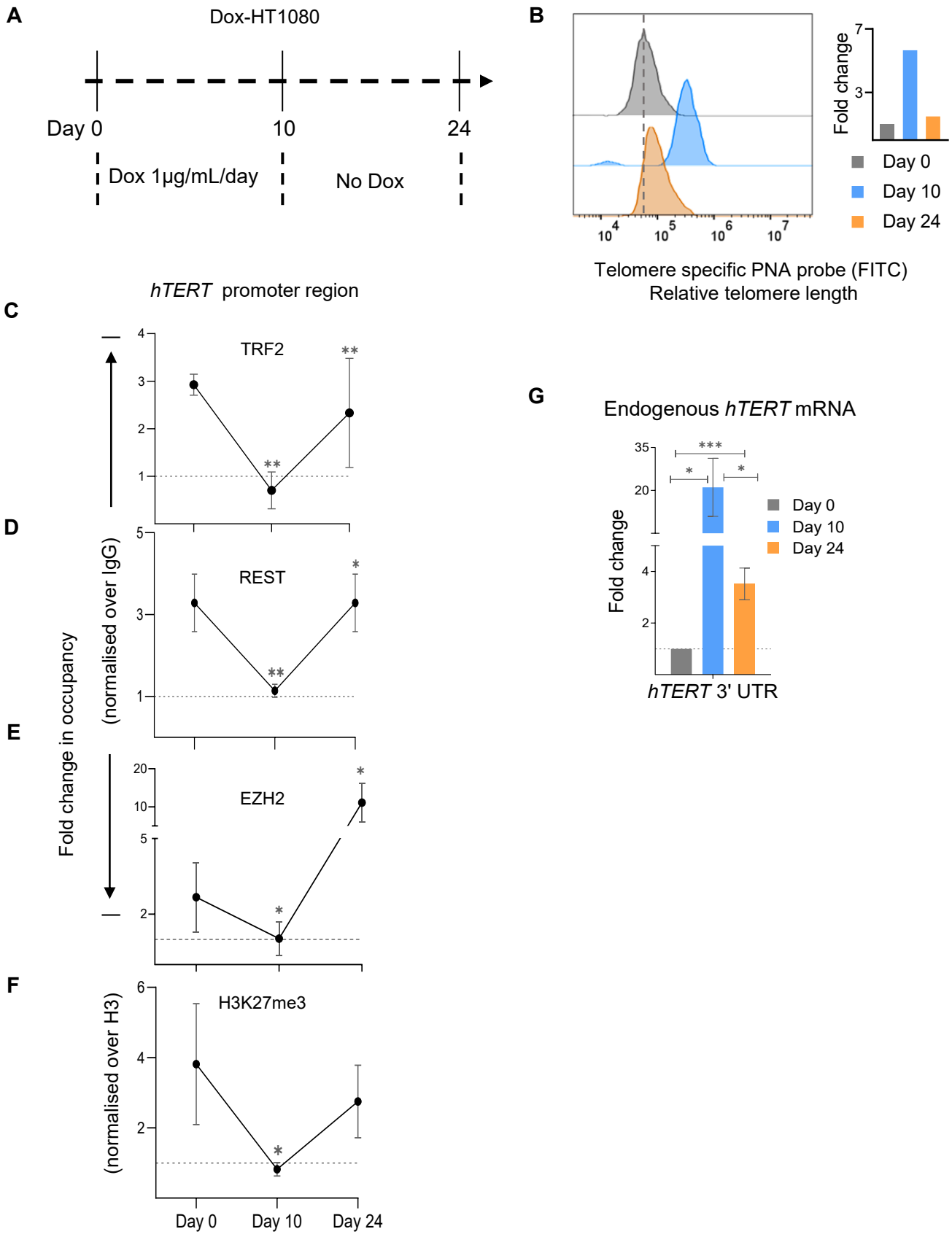
A
Dox-HT1080
Day 0
10
24
Dox 1µg/mL/day
No Dox
B
Fold change
Day 0
Day 10
Day 24
Telomere specific PNA probe (FITC)
Relative telomere length
C
hTERT promoter region
TRF2
D
REST
E
EZH2
F
H3K27me3
Fold change in occupancy
(normalised over IgG)
(normalised over H3)
Day 0
Day 10
Day 24
G
Endogenous hTERT mRNA
Fold change
hTERT 3' UTR

Figure 3.

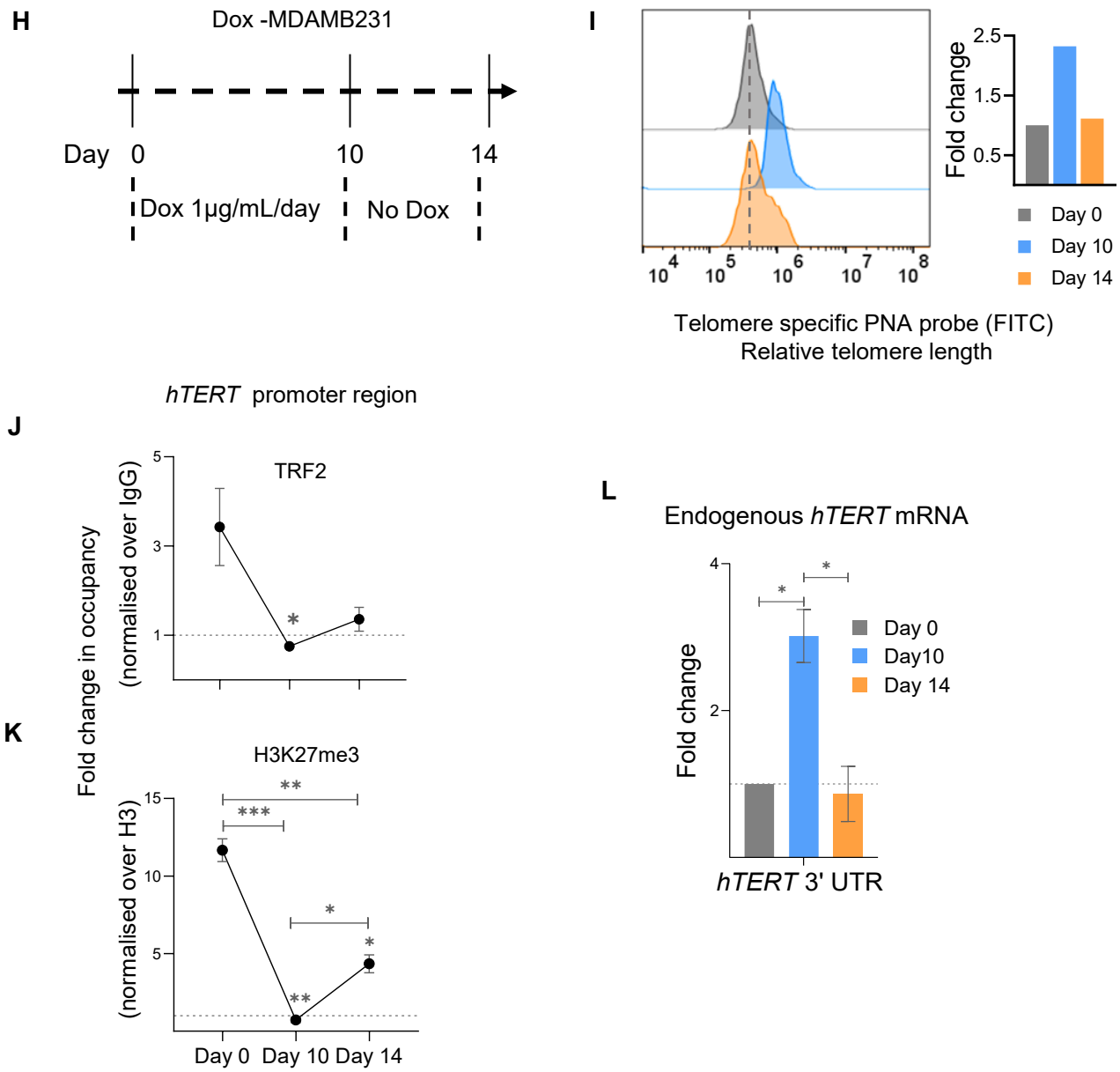

Figure 3. Temporal telomere length elongation followed by shortening shows telomeresensitive transcriptional regulation of *hTERT*

(A) Scheme depicting protocol followed for doxycycline (Dox) inducible hTERT overexpression in HT1080 cells (Dox-HT1080)

(B) Relative fold change in telomere length at day intervals (as indicated) determinedby FACS in Dox-HT1080 cells; quantification in right panel

(C-F) ChIP followed by qRT-PCR at the *hTERT* promoter for TRF2 (C), REST (D), EZH2 (E) or H3K27me3 (F) in Dox-HT1080 cells at Day 0,10 and 24; occupancy normalized to respective IgG or total Histone H3 (for H3K27me3)

(G) *hTERT* mRNA expression by qRT-PCR using hTERT specific 3'UTR primers in Dox- HT1080 cells at day intervals (as indicated); normalized to *GAPDH* mRNA levels

(H) Scheme depicting protocol followed for doxycycline (Dox) inducible hTERT overexpression in MDAMB231 (Dox-MDAMB231)

(I) Relative fold change in telomere length at multiple day intervals (as indicated) determined by Flow cytometry in Dox-MDAMB231; quantification in right panel

(J, K) ChIP followed by qRT-PCR at the *hTERT* promoter for TRF2 (J) and H3K27me3 (K) in Dox-MDAMB231 cells at at Day 0,10 and 14; occupancy normalized to respective IgG or total Histone H3 (for H3K27me3)

(L) *hTERT* mRNA expression by qRT-PCR using hTERT specific 3'UTR primer in Dox- MDAMB231 cells at day intervals (as indicated); normalized to *GAPDH* mRNA levels

Error bars represent ± SDs from mean. p values are calculated by paired/unpaired t test and one way ANOVA in C-F, J, K (*$p < 0.05$, **$p < 0.01$, ***$p < 0.005$, ****$p < 0.0001$)

Figure 4.

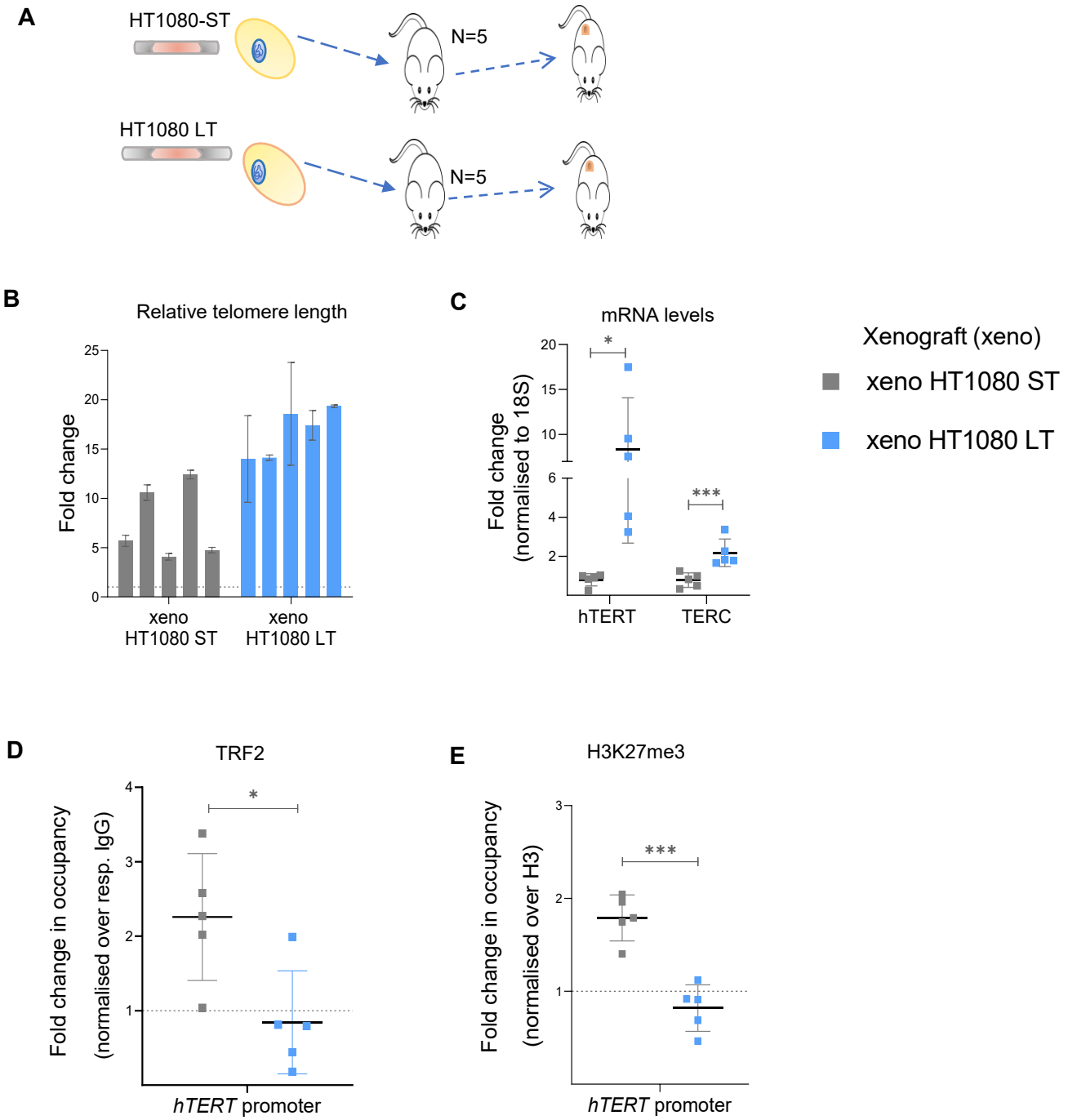
A
HT1080-ST
N=5
HT1080 LT
N=5
B
Relative telomere length
Fold change
25
20
15
10
5
0
xeno HT1080 ST
xeno HT1080 LT
C
mRNA levels
Fold change (normalised to 18S)
20
15
10
6
4
2
*
***
hTERT
TERC
Xenograft (xeno)
xeno HT1080 ST
xeno HT1080 LT
D
TRF2
Fold change in occupancy (normalised over resp. IgG)
4
3
2
1
*
hTERT promoter
E
H3K27me3
Fold change in occupancy (normalised over H3)
3
2
1
***
hTERT promoter

Figure 4. Telomere length sensitive *hTERT* regulation in *in vivo* tumour xenografts

(A) Scheme depicting the generation of tumour xenograft with HT1080-ST or HT1080-LT cells

(B) Relative fold change in telomere length in xenograft samples determined by qRT- PCR- based telomere length detection method as reported earlier (O'Callaghan et al., 2008 and Cawthon et al 2002). Telomeric signal normalised over single copy gene, 36B4

(C) *hTERT* (exon 15/16 full length transcript) and *hTERC* mRNA expression in xenograft tissues by qRT-PCR; normalized to 18S mRNA levels

(D, E) ChIP followed by qPCR at the *hTERT* promoter for TRF2 (D) and H3K27me3 (E); occupancy normalized to respective IgG and total H3 (for H3K27me3)

Error bars represent ± SDs from mean. p values are calculated by paired/unpaired t test (*$p < 0.05$, **$p < 0.01$, ***$p < 0.005$, ****$p < 0.0001$)

Figure 5.

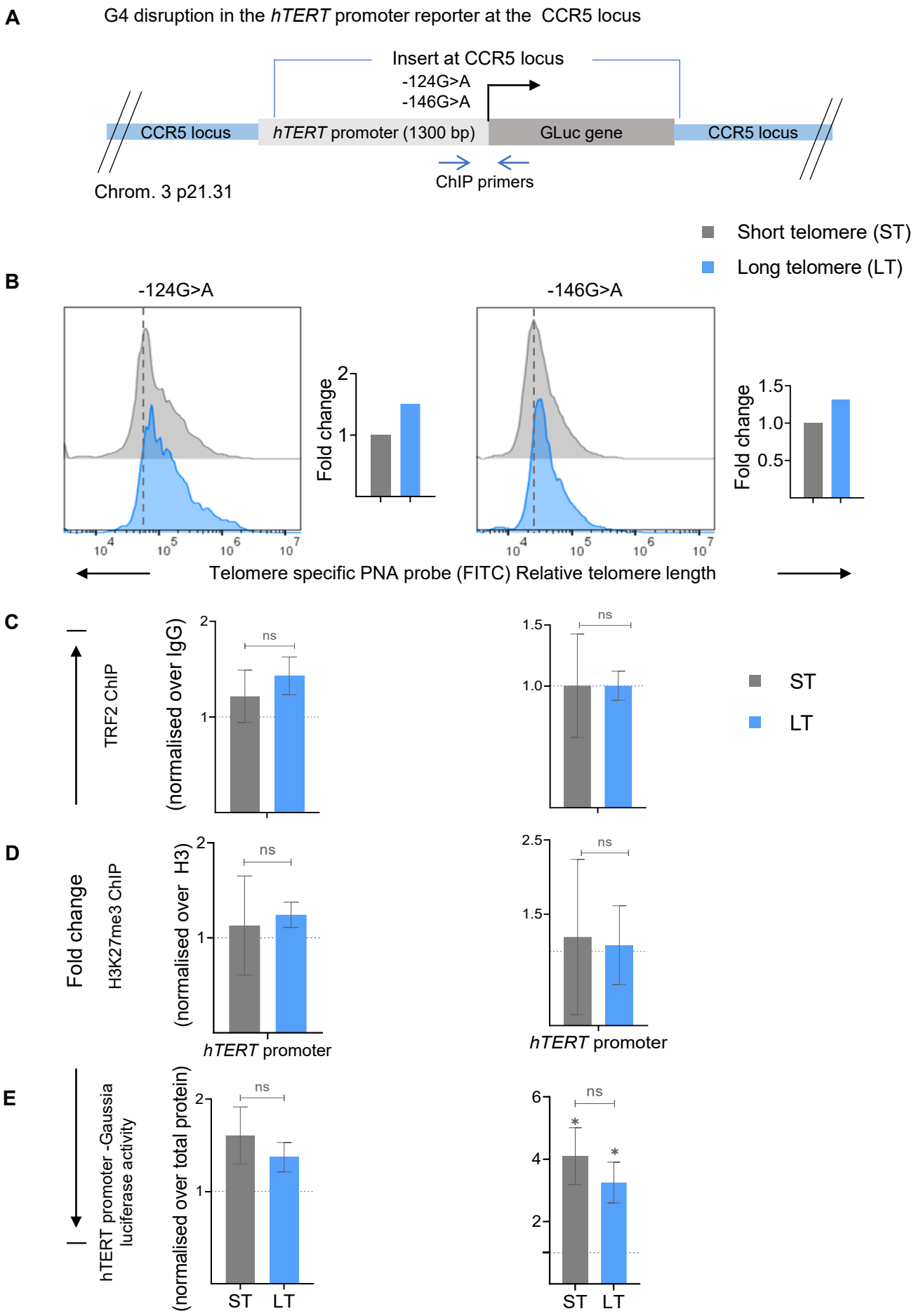
A
G4 disruption in the hTERT promoter reporter at the CCR5 locus
Insert at CCR5 locus
-124G>A
-146G>A
CCR5 locus
hTERT promoter (1300 bp)
GLuc gene
CCR5 locus
ChIP primers
Chrom. 3 p21.31
Short telomere (ST)
Long telomere (LT)
B
-124G>A
-146G>A
Fold change
Telomere specific PNA probe (FITC) Relative telomere length
C
TRF2 ChIP
(normalised over IgG)
ns
ST
LT
D
Fold change
H3K27me3 ChIP
(normalised over H3)
hTERT promoter
E
hTERT promoter -Gaussia luciferase activity
(normalised over total protein)
ST
LT

Figure 5. G-quadruplex mediated TRF2 binding is essential for telomere-dependent hTERT regulation

(A) Scheme depicting CRISPR modified HEK293T cells with 1300 bp *hTERT* promoter with G>A substitution at -124 or -146 bp (upstream of TSS) driving gaussia luciferase (gluc) construct at the CCR5 safe harbor locus. Scheme denotes ChIP primers used to study chromatin occupancy of 0-300 bp *hTERT* promoter region inserted at the exogenous locus

(B) Relative fold change in telomere length in two independent pairs of cells with short or long telomeres containing *hTERT* promoter G4 disrupting mutations (-124G>A or - 146G>A) at CCR5 locus *hTERT* promoter insert as determined by Flow cytometry; quantification in right panel

(C, D) ChIP followed by qRT-PCR at the inserted *hTERT* promoter (0-300 bp upstream of TSS) for TRF2 (C), and H3K27me3 (D) in pairs of cells generated with -124G>A or -146G>A mutation with long/ short telomeres. Occupancy normalized to respective IgG or total histone H3 (for H3K27me3)

(E) *hTERT* promoter-gaussia luciferase activity in short or long telomere cells with - 124G>A and -146G>A mutated *hTERT* promoter sequence. Reporter activity normalized to respective total protein levels. Fold change have been calculated over unmutated promoter-gluc LT cells (Figure 1L) for all cases.

Error bars represent ± SDs from mean. p values are calculated by paired/unpaired t test (*$p < 0.05$, **$p < 0.01$, ***$p < 0.005$, ****$p < 0.0001$)

Figure 6.

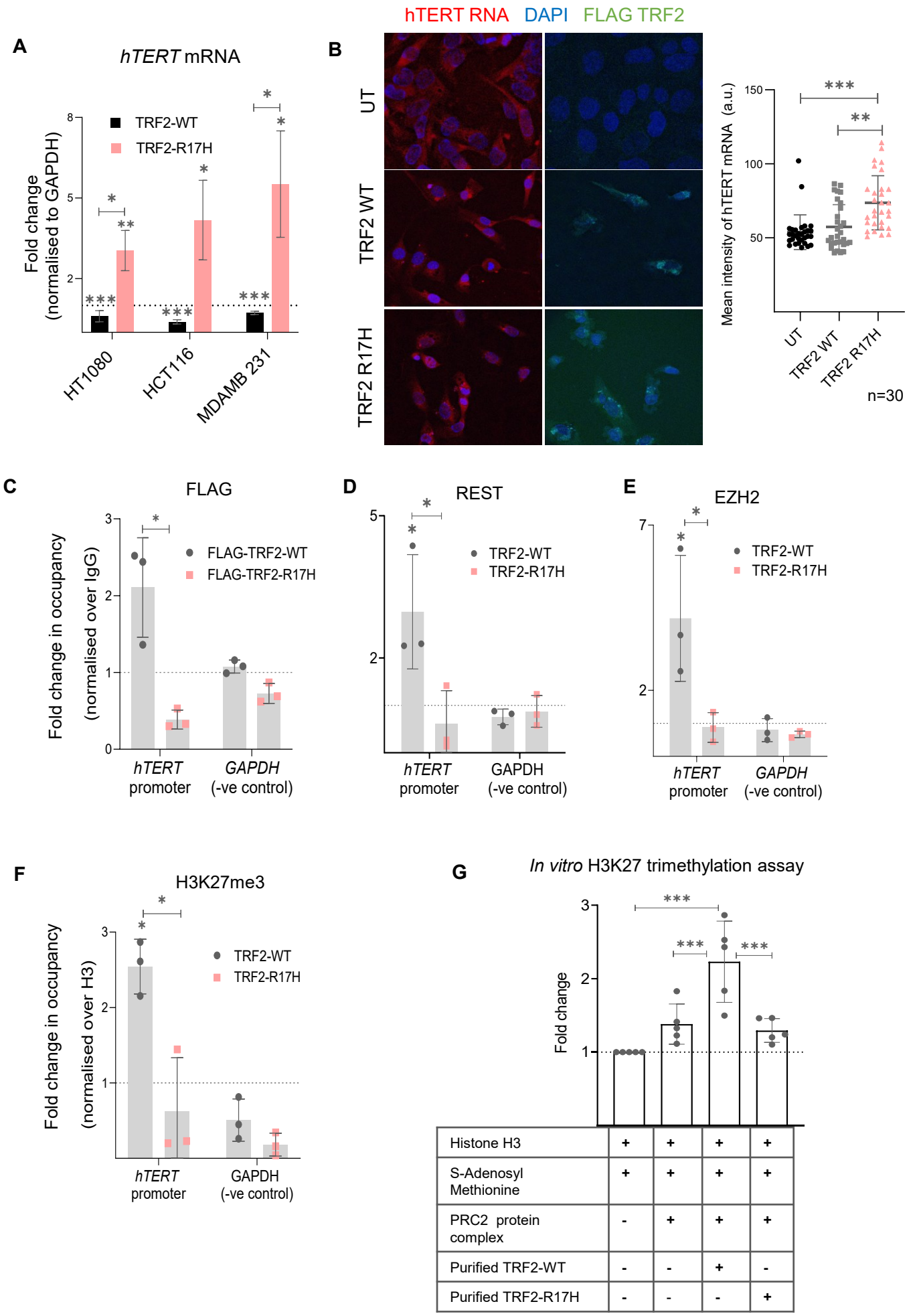
A
hTERT mRNA
TRF2-WT
TRF2-R17H
Fold change (normalised to GAPDH)
HT1080
HCT116
MDAMB 231
B
hTERT RNA
DAPI
FLAG TRF2
UT
TRF2 WT
TRF2 R17H
Mean intensity of hTERT mRNA (a.u.)
n=30
C
FLAG
FLAG-TRF2-WT
FLAG-TRF2-R17H
Fold change in occupancy (normalised over IgG)
hTERT promoter
GAPDH (-ve control)
D
REST
TRF2-WT
TRF2-R17H
E
EZH2
F
H3K27me3
Fold change in occupancy (normalised over H3)
G
In vitro H3K27 trimethylation assay
Fold change
Histone H3
S-Adenosyl Methionine
PRC2 protein complex
Purified TRF2-WT
Purified TRF2-R17H

Figure 6. TRF2 R17 methylation is essential for repression of *hTERT* transcription

(A) hTERT full length transcript (exon 15/16) mRNA expression levels by qRT-PCR; normalized to GAPDH mRNA levels upon stable doxycycline induction of wildtype (WT) TRF2 or R17H TRF2 mutants in HT1080, HCT116 or MDAMB231 cells

(B) *hTERT* mRNA FISH upon TRF2 WT or TRF2 R17H overexpression (untransfected, UT as control) in HT1080 cells; quantification shown in right panel

(C-F) ChIP followed by qRT-PCR at the hTERT promoter for FLAG-tagged TRF2 (C), REST (D), EZH2 (E) or H3K27me3 (F) in HT1080 cells upon expression of WT TRF2 or TRF2 R17H. Occupancy normalized to respective IgG and total Histone H3 (for H3K27me3); qRT-PCR on *GAPDH* promoter used as negative control in all cases.

(G) *In vitro* methyl transferase activity of the reconstituted PRC2 complex resulting inH3K27 trimethylation in presence or absence of TRF2 WT or TRF2 R17H protein.

Error bars represent ± SDs from mean. p values are calculated by paired/unpaired t test and two-way ANOVA in (G) (*$p < 0.05$, **$p < 0.01$, ***$p < 0.005$, ****$p < 0.0001$)

Figure 7.

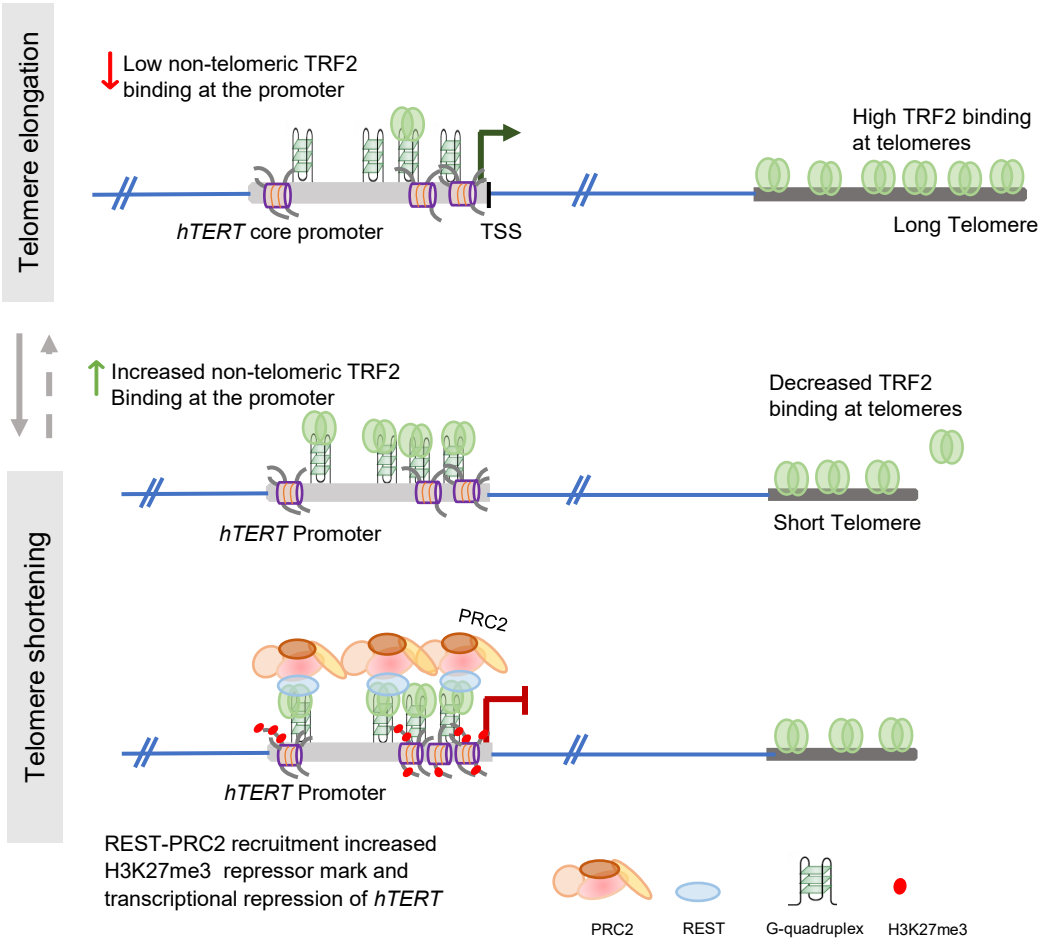

Figure 7. Telomere length controls human Telomerase (*hTERT*) expression through Non-Telomeric TRF2

The figure illustrates the telomere-dependent epigenetic modification of chromatin structure at the *hTERT* promoter, resulting in upregulation or downregulation of *hTERT* expression due to altered non-telomeric TRF2 binding at the promoter. Relatively long telomeres cells (top panel) have lower TRF2 binding at *hTERT* promoter, promoting permissive chromatin and upregulation of *hTERT* transcription. Conversely, shorter telomeres cells (bottom panel) with increased TRF2 binding at *hTERT* promoter recruit more REST-PRC2 epigenetic complex causing increased repressor histone H3K27 trimethylation deposition. This leads to a more closed chromatin state at the *hTERT* promoter, suppressing hTERT transcription.